

# Catalytic glycosylation for minimally protected donors and acceptors

<https://doi.org/10.1038/s41586-024-07695-4>

Received: 1 March 2024

Accepted: 7 June 2024

Published online: 17 June 2024

 Check for updates

Qiu-Di Dang<sup>1,4</sup>, Yi-Hui Deng<sup>2,3,4</sup>, Tian-Yu Sun<sup>2,3</sup>, Yao Zhang<sup>1</sup>, Jun Li<sup>1</sup>, Xia Zhang<sup>1</sup>, Yun-Dong Wu<sup>2,3</sup> & Dawen Niu<sup>1</sup><sup>✉</sup>

Oligosaccharides have myriad functions throughout biological processes<sup>1,2</sup>. Chemical synthesis of these structurally complex molecules facilitates investigation of their functions. With a dense concentration of stereocentres and hydroxyl groups, oligosaccharide assembly through *O*-glycosylation requires simultaneous control of site, stereo- and chemoselectivities<sup>3,4</sup>. Chemists have traditionally relied on protecting group manipulations for this purpose<sup>5–8</sup>, adding considerable synthetic work. Here we report a glycosylation platform that enables selective coupling between unprotected or minimally protected donor and acceptor sugars, producing 1,2-*cis*-*O*-glycosides in a catalyst-controlled, site-selective manner. Radical-based activation<sup>9</sup> of allyl glycosyl sulfones forms glycosyl bromides. A designed aminoboronic acid catalyst brings this reactive intermediate close to an acceptor through a network of non-covalent hydrogen bonding and reversible covalent B–O bonding interactions, allowing precise glycosyl transfer. The site of glycosylation can be switched with different aminoboronic acid catalysts by affecting their interaction modes with substrates. The method accommodates a wide range of sugar types, amenable to the preparation of naturally occurring sugar chains and pentasaccharides containing 11 free hydroxyls. Experimental and computational studies provide insights into the origin of selectivity outcomes.

Oligosaccharide assembly involves stereocontrolled C–O bond formation between an anomeric carbon centre and one of many hydroxyl groups, a major challenge in chemistry<sup>3,4</sup>. As briefly illustrated in Fig. 1a, given the number of free hydroxyl groups present in both reactants, and considering the two possible configurations ( $\alpha$  and  $\beta$ ) of the resulting anomeric (glycosidic) centre, the reaction between glycosyl donor **1** and acceptor **2** could potentially afford a total of  $(m + n + 1) \times 2$  disaccharide products. To obtain only one of these (for example, **3**) efficiently, methods that can simultaneously address site, stereo- and chemoselectivity issues are demanded. For over a century, chemists have mostly resorted to the use of ‘protecting’ groups (**4** + **5** to **6** to **3**) to tackle such challenges<sup>5–8</sup>. In fact, the roles of certain protecting groups include both blocking of unwanted reaction sites and controlling stereoselectivity. Notable achievements have been made, allowing the preparation of complex oligosaccharides<sup>10–14</sup>. Regardless, overturning the dominance of protecting groups<sup>15–18</sup> still represents one of the most actively sought-after goals. Advancements in this direction would not only streamline the synthesis of oligosaccharides, but also avoid potential problems related to deprotection of the final products. More importantly, it may open new horizons for selectivity control, providing products difficult to access by conventional, protecting-group-based approaches. Towards this end, milestones include the methods from the Aoyama<sup>19</sup>, Taylor<sup>20,21</sup>, and Toshima<sup>22,23</sup> groups that use boronic/borinic acid catalysts; from the Jacobsen

group<sup>24,25</sup> that exploits bis-urea catalysts; from the Miller group<sup>26,27</sup> that explores Ca<sup>2+</sup>/sucrose complexation; from the Loh group that harnesses various non-covalent interactions<sup>28</sup>; and from others selectively modifying sugars<sup>16–18,29–33</sup>. However, these reported methods either still require fully protected glycosyl donors or show limited substrate scope. A generally applicable, selective glycosylation platform for coupling of minimally protected donors and acceptors remains elusive. Even more demanding is to switch product selectivity through catalyst control.

With the goal of developing selective *O*-glycosylation methods that minimize reliance on protecting groups but use catalyst control, we proposed the strategy depicted in Fig. 1b. We recently established a radical-based approach that converts bench-stable and readily available allyl glycosyl sulfones to reactive glycosyl electrophiles<sup>9,34</sup> (**7** to **8**). Because this donor activation method demonstrates compatibility with most polar functional groups—including free hydroxyl groups—we reason that it would grant sufficient working space for unprotected substrates and delicate catalysts. We posited that, if we could deploy catalysts such as **9** that can knit together nucleophilic acceptor **2** and electrophilic donor **8**—presumably through multiple non-covalent or reversible covalent interactions (Fig. 1b, dashed lines)—selective *O*-glycosylation between minimally protected reactants to form **3** might be achieved. However, for such a design to work the following requirements must also be satisfied. First, the catalyst

<sup>1</sup>State Key Laboratory of Biotherapy and Cancer Center, West China Hospital and School of Chemical Engineering, Sichuan University, Chengdu, China. <sup>2</sup>The Key Laboratory of Computational Chemistry and Drug Design, State Key Laboratory of Chemical Oncogenomic, School of Chemical Biology and Biotechnology, Peking University Shenzhen Graduate School, Shenzhen, China. <sup>3</sup>Institute of Molecular Chemical Biology, Shenzhen Bay Laboratory, Shenzhen, China. <sup>4</sup>These authors contributed equally: Qiu-Di Dang, Yi-Hui Deng. <sup>✉</sup>e-mail: wuyd@pkusz.edu.cn; niudawen@scu.edu.cn

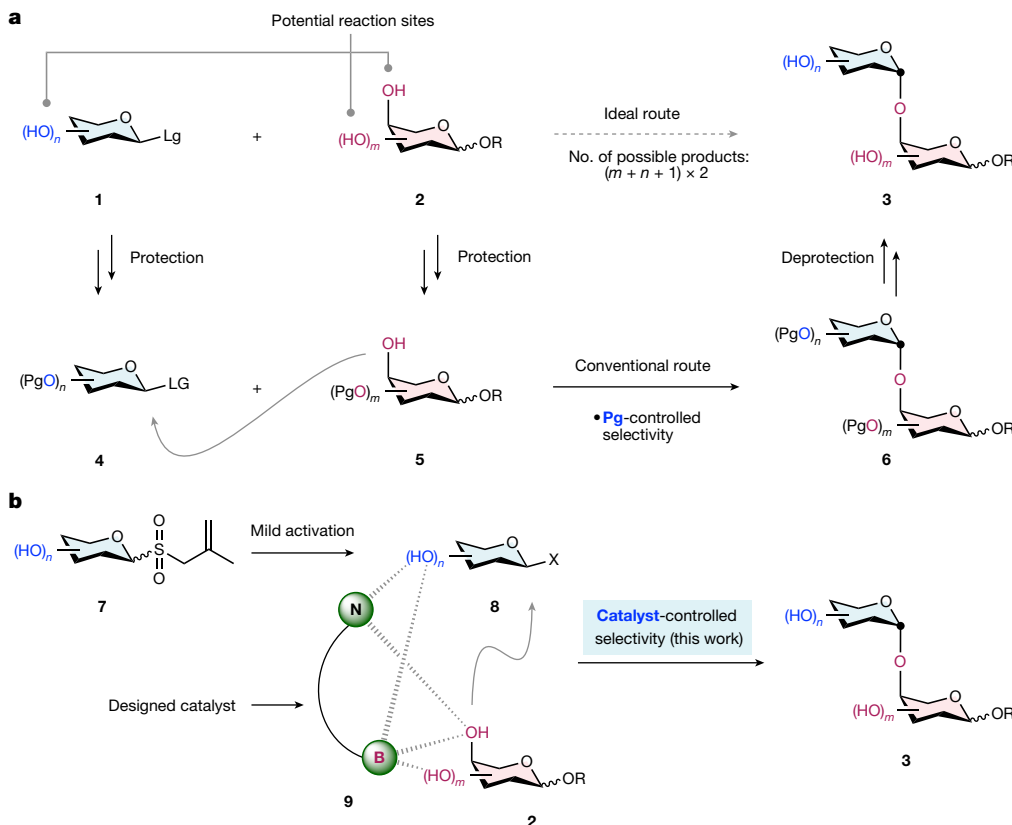


**Fig. 1 | Oligosaccharide synthesis: background, approaches and our reaction design.** **a**, Ideal and conventional chemical approaches for construction of glycosidic bonds. **b**, Catalyst-controlled, selective *O*-glycosylation between

minimally protected donors and acceptors (this work). Lg, leaving group; Pg, protecting group.

to be identified should not interfere with the donor activation process. Second, the unprotected, reactive intermediate **8** should be sufficiently long-lived to be recognized by the catalyst before it undergoes non-productive decomposition. Third, the catalyst should orient both reactants (**8** and **2**) in a precise way to ensure good site and stereoselectivity. Fourth, oligosaccharide product **3**, following its formation, should not occupy the catalyst for too long and thereby inhibit its function (that is, product inhibition).

Despite the above obstacles, we have shown the viability of such a strategy. It allows the development of general *O*-glycosylation methods with selectivity profiles difficult to achieve by approaches based on protecting groups. Moreover, the site of glycosylation can be altered simply through modification of catalyst structures, thereby accomplishing catalyst-controlled site divergency<sup>35,36</sup>. The utility of the method is further demonstrated by the rapid synthesis of naturally occurring oligosaccharides. Experimental and computational studies provide insights into the origin of selectivities, which results from a network of non-covalent and reversible covalent interactions between catalysts and substrates.

## Reaction validation

We commenced our study using donor **10** (derived from glucose) and acceptor **11** (derived from fucose) as model substrates, with the aim of making disaccharide products such as **12a/b** (Fig. 2). Both reactants are minimally protected, containing five free hydroxyls in total. As expected<sup>9,34</sup>, sulfone donor **10** could be converted to the corresponding glycosyl bromide **14** (presumably in equilibrium<sup>37</sup> with its epimer **15**) via **13** by visible-light irradiation (455 nm) in the presence of *fac*-Ir(ppy)<sub>3</sub> and BrCF<sub>3</sub>CO<sub>2</sub>Et (see Extended Data Fig. 1 for the proposed pathway). According to our design in Fig. 1b, because a catalyst hosting both **11**

and **15** is needed, we designed catalysts with the general structure of **16** containing two functional units—a boronic acid and an amine moiety—that are linked by a C–N bond. The boronic acid group will recognize and chelate with various sugar acceptors possessing *cis*-1,2-diol units, and such boron–sugar interaction has been widely applied in sensing, biological sciences<sup>38,39</sup> and synthetic chemistry<sup>19–23,30,31</sup>. As an important structural feature, the amine groups in **16** are intended to provide additional docking sites for hydroxyl groups abundant in both reactants through non-covalent hydrogen bonding interactions<sup>40</sup>. Notably, such designed catalysts can be readily prepared by reductive amination and their structures readily tuned through the use of different building blocks.

Through extensive optimization (see Supplementary Tables 1–4 for additional data), we identified aminoboronic acid catalysts **16K/L** that enabled direct reaction between **10** (1.0 equiv.) and **11** (1.5 equiv.) to give **12a** in a highly selective manner. The reaction proceeds with ethyl acetate as solvent at room temperature (about 25 °C) and under almost neutral conditions [(NH<sub>4</sub>)<sub>2</sub>HPO<sub>4</sub>]. Among the solvents we examined (Supplementary Table 3), low-toxic ethyl acetate appeared to be optimal probably because it offers reasonable solubility to both substrates without significantly impeding their interactions with the catalyst. The following two features of the reaction are particularly salient. In terms of stereoselectivity, the 1,2-*cis* glycosidic linkage—often considered more difficult<sup>41,42</sup> to build than its 1,2-*trans* counterpart—is formed almost exclusively. In terms of site selectivity, the one undergoing glycosylation is the axial C4-OH of acceptor **11**, intrinsically the least nucleophilic<sup>43,44</sup> of all three secondary hydroxyls in the fucose backbone. Such selectivity profile is rather unexpected and would be difficult to achieve using conventional approaches.

Catalysts played indispensable roles in this reaction; in the absence of a catalyst, donor **10** fully decomposed to intractable mixtures. We

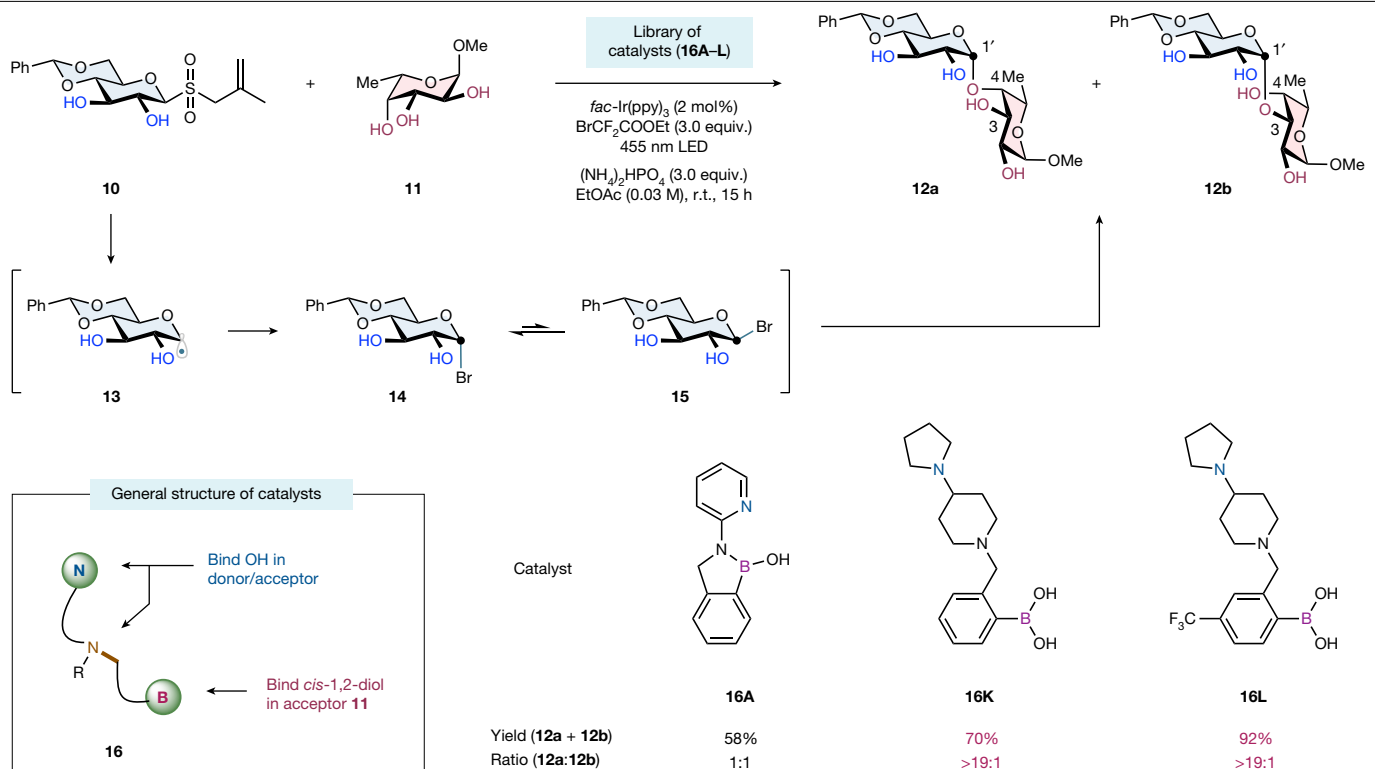


**Fig. 2 | Reaction validation and condition optimization.** The model reaction uses minimally protected donor **10** and acceptor **11**. Product ratios were determined by <sup>1</sup>H NMR analysis of the crude reaction mixture. Reactions were

performed at 0.05 mmol scale in EtOAc (0.03 M) for 15 h using *fac*-Ir(ppy)<sub>3</sub> (2 mol%), BrCF<sub>2</sub>COOEt (3.0 equiv.), (NH<sub>4</sub>)<sub>2</sub>HPO<sub>4</sub> (3.0 equiv.) and a catalyst (0.2 equiv.). LED, light-emitting diode; r.t., room temperature.

attempted to use a number of simple boronic/borinic acid catalysts previously reported for selective modification of sugars<sup>19–23</sup> but obtained no detectable level of product in this context (Supplementary Table 4). As shown in Extended Data Fig. 2, pyridine-based catalysts (**16A–F**) enabled product formation, albeit with poor site selectivity (**12a**:**12b** ratio). From these results we noted that the presence of a N atom in the pyridine ring (compare **16A** with **16E**) and its position relative to the boron centre (compare **16A** with **16B–D**) are critical for the performance of these catalysts. We further designed and examined piperidine-based catalysts **16G–L**, eventually finding that **16K/L** provided excellent control over site, chemo- and stereoselectivity. Truncating the pyrrolidine ring in **16K/L** (compare with **16G/H**) or substituting it with other groups (compare with **16I/J**) resulted in diminished yield and selectivity, again suggesting non-covalent interactions between the amine groups in **16K/L** and OH groups in reactants. Electronic perturbation of the aryl backbone is allowed: the CF<sub>3</sub>-substituted catalyst **16L** gave a higher yield of **12a** than did **16K**, probably due to the enhanced Lewis acidity (oxophilicity) of its boron centre.

## Substrate scope

With proof of concept validated, we proceeded to explore the generality of this method (Fig. 3). Most of the examples shown in Fig. 3 were prepared using either **16K** or **16L** as catalyst. Due to a catalyst-controlled (rather than substrate-controlled) mechanism, the reaction exhibited minimal sensitivity to substrate properties, a rare but desired feature in carbohydrate synthesis<sup>45</sup>. As shown in the top three rows of Fig. 3, various donors derived from monosaccharides such as glucose (**17a,b**), galactose (**17c**), fucose (**18d**) and arabinose (**18c**) partook in this reaction smoothly. For donors containing the *cis*-1,2-diol unit, one of the two hydroxyl groups needs to be capped to avoid potential competition with acceptors for the aminoboronic acid catalyst. The silyl (**17b,c**),

ester (**17c**) or benzylidene groups (**17a**) in donors are all tolerated. More complex disaccharide donors can be used, as exemplified by the synthesis of **18e,f**. In addition to the 1,2-*cis*- $\alpha$ -glycosidic linkages in the above cases, this method could also be applied in the construction of the more challenging<sup>46</sup> 1,2-*cis*- $\beta$ -linkages (**19,20**). We attribute this high 1,2-*cis* selectivity to the coordination of C2-OH in the donor with the boron atom in the catalyst, which facilitates intramolecular glycosyl transfer<sup>22,23</sup> to the acceptor in a 1,2-*cis* manner. Minimal background glycosylation occurring without catalyst may also contribute to the high stereoselectivity observed.

A wide range of acceptors are accommodated. Those bearing *cis*-1,2-diol units—such as galactose (**17a–f**), rhamnose (**18a–f**), mannose (**19,21**), fucose (**20**), arabinose (**22**), lyxose (**23**) and fructose (**24**)—all underwent this reaction efficiently. The anomeric configuration of acceptors is inconsequential (**17a–c** versus **17d–f**). Phenolic O-glycosides (**17f**) can be used. Both O- and S-glycosides (**17e**) are allowed. For the above acceptors, the glycosyl units are installed onto the (often intrinsically least reactive) axial hydroxyl group with good site selectivity, another hallmark of this method.

Our method is not restricted to acceptors containing *cis*-1,2-diols, as exemplified by the successful engagement of sucrose-derived acceptors as substrates (**25**). We speculated that the C2-OH and C2'-OH in **25** could effectively chelate with the boron centre of the catalyst (see Supplementary Information Section 10 for a computed structure of this complex), enabling the formation of a ternary complex like that shown in Fig. 1b. Lastly, a shikimic acid ester containing three consecutive hydroxyls was involved in this reaction (**26**), suggesting that this method can also be extended to non-sugar acceptors. To date, attempts to engage the 4,6-diols of glucopyranosides as acceptors in our reaction resulted in non-selective outcomes.

More complex oligosaccharides can be prepared. As shown in the bottom two rows of Fig. 3, the method was successfully adopted in

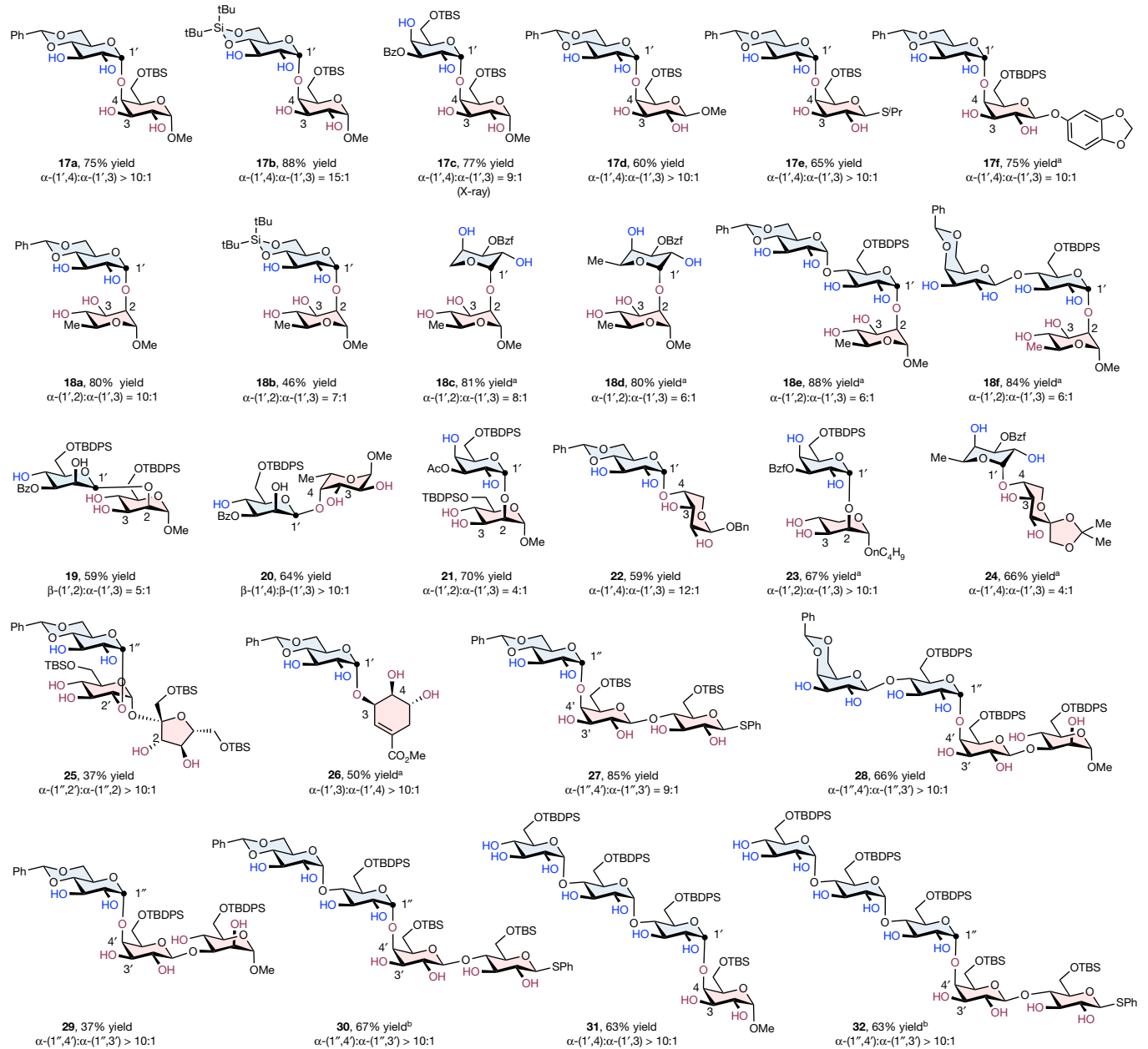


**Fig. 3 | Scope of donors and acceptors.** Unless otherwise noted, reactions in this figure were performed at 0.1 or 0.2 mmol scale in EtOAc (0.03 M) for 15 h using donor (1.0 equiv.), acceptor (1.5–2.0 equiv.), *fac*-Ir(ppy)<sub>3</sub> (2 mol%), BrCF<sub>2</sub>CO<sub>2</sub>Et (3.0 equiv.), (NH<sub>4</sub>)<sub>2</sub>HPO<sub>4</sub> (3.0 equiv.) and aminoboronic acid catalyst

**16K** (0.2 equiv.). Product ratios were determined by <sup>1</sup>H NMR analysis of the crude reaction mixture. Isolated yields are reported. <sup>a</sup>16L was used as catalyst.

<sup>b</sup>16A was used as catalyst. See Supplementary Information for experimental details. Bz, benzoyl; Bzf, 4-(trifluoromethyl)benzoyl; iPr, isopropyl.

[2 + 2], [3 + 1] and [3 + 2] couplings to make tetra- or pentasaccharides (**27–32**). Notably, product **32**, which contains 11 free hydroxyl groups, was formed in an efficient and selective manner.

### Site-divergent glycosylation

Simply through structural alteration of catalysts, this platform allowed catalyst-controlled, site-divergent *O*-glycosylation (Fig. 4a). Taking fucose-derived acceptor **11** as an example, whereas the use of catalyst **16K** resulted in glycosylation of axial C4-OH within its *cis*-1,2-diol motif (left arrow), catalyst **16M**<sup>47</sup> directed the glycosyl group to the equatorial C3-OH (right arrow). In both cases the 1,2-*cis*-configured glycosidic bond was formed selectively. Such site divergence shows good generality and

also operates for lyxose (**33a/b**), fructose (**34a/b**), arabinose (**35a/b**) and mannose acceptors (**37–40**). On the other hand, donors derived from glucoses (**37a/b**), glucuronates (**38a/b**), galactoses (**39a/b**) and disaccharides such as lactose (**40a/b**) can be installed onto the mannose-derived acceptor **36a** or **36b** in a site-divergent manner. We would like to emphasize that achieving site-selective *O*-glycosylation of sugars has already presented a notable challenge<sup>16–18,25</sup>, and developing a site-divergent version is even more demanding and has seen little progress thus far. Our work has advanced this area using designed catalysts in the context of minimally protected donors and acceptors.

To further demonstrate the utility of this method, we applied it in the preparation of naturally occurring oligosaccharide chains (Extended Data Fig. 3). Globosides are a subclass of glycosphingolipids, with a

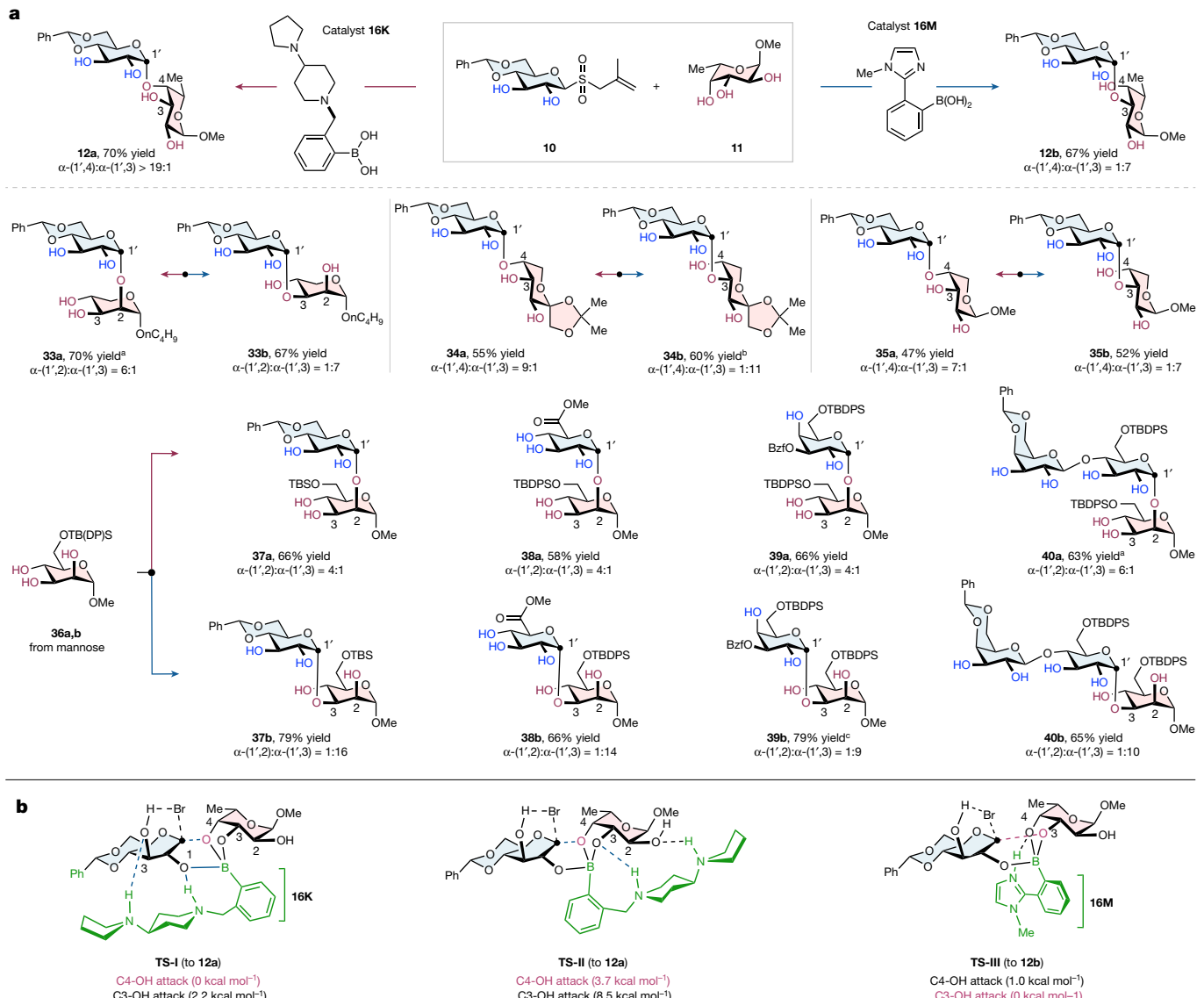


**Fig. 4 | Site-divergent glycosylation and mechanistic rationale for selectivity switch.** **a**, Scope of catalyst-controlled, site-divergent glycosylation. Unless otherwise noted, reactions in this figure were performed at 0.1 or 0.2 mmol scale in EtOAc (0.03 M) for 15 h using *fac*-Ir(ppy)<sub>3</sub> (2 mol%), BrCF<sub>2</sub>CO<sub>2</sub>Et (3.0 equiv.), (NH<sub>4</sub>)<sub>2</sub>HPO<sub>4</sub> (3.0 equiv.), **16K** (0.2 equiv. for red arrow) and **16A** (0.2 equiv. for blue arrow). Product ratios were determined by <sup>1</sup>H NMR analysis of the crude reaction mixture. Isolated yields are reported.

See Supplementary Information for experimental details. **b**, Transition structures (TS) rationalizing the selectivity switch. DFT calculations were performed at the B3LYP-D3(BJ)/def2TZVPP/SMD(EtOAc)//B3LYP-D3(BJ)/6-31G(d,p) level of theory. See Supplementary Information Section 10 for experimental and computational details. <sup>a</sup>**16L** used as catalyst. <sup>b</sup>**16F** used as catalyst. <sup>c</sup>**16N** used as catalyst.

common core trisaccharide unit of Gal $\alpha$ 1,4Gal $\beta$ 1,4Glc $\beta$ . By our method, this unit (see **43**) can be made from galactose-derived donor **41** and lactose-derived acceptor **42** with the aid of catalyst **16L**. Note that product **43** contains six unprotected hydroxyls. Trisaccharide **47** is related to the repeating unit found in *Klebsiella* K20. Treating **44** with **36b** in the presence of catalyst **16N** gave 1,2-cis-linked disaccharide **45** following ester hydrolysis. The resulting disaccharide **45** then reacted with protected glucosyl bromide **46** in the presence of catalyst **16A** and Ag<sub>2</sub>CO<sub>3</sub> to yield trisaccharide **47**.

## Mechanism

To probe the origin of selectivities we first performed control experiments using donors/acceptors with perturbed structures (**10a–c** and **11a**; Extended Data Fig. 4a). In stark contrast to **10**, neither donor **10a** (C2-OH methylated) nor **10b** (C2-OH removed) delivered a detectable

amount of product when subjected to our standard conditions (central box). In these cases, byproduct **48** or **49** was formed. These results highlight the essential role of the unprotected C2-OH group in **10**. On the other hand, methylation of the C3-OH in donor **10** (**10c**, left box) and removal of C2-OH in acceptor **11** (**11a**, right box) had moderate to minimal effects on selectivity but diminished product yield.

We then investigated the identity of key reaction intermediates. As alluded to in Fig. 2, glycosyl bromides (such as **14/15**) formed in situ probably serve as the reactive sugar donors (see Extended Data Fig. 5 for support). For acceptors, we found that the addition of **11** caused a new peak in the <sup>11</sup>B nuclear magnetic resonance (NMR) spectrum of **16K** and improved the solubility of **16M** (Extended Data Fig. 4b), suggesting that they readily form complexes with aminoboronic acid catalysts. Such complexation would enhance the nucleophilicity of sugar acceptors<sup>20,21</sup> and prime them for the subsequent glycosidic bond-forming step.

# Article

With the above information we used density functional theory (DFT) calculations to examine how our catalysts functioned, using bromide **14/15** and complex **16K + 11** or **16M + 11** as model partners. Key transition structures **TS-I – III** are shown in Fig. 4b (see Supplementary Information Section 10 for other, energetically less favoured, pathways and structures). They share the following features. First, as in Lemieux glycosylation<sup>37,48</sup>, equatorial glycosyl bromide **15** acts as the electrophile (Extended Data Fig. 6). Second, as anticipated, aminoboronic acid catalysts bring donors and acceptors into closer proximity. Third, consistent with its crucial role in reaction efficiency (Extended Data Fig. 4a), the C2-OH in donor **15** coordinates with the boron atom in our catalysts, assisting the delivery of acceptors in a 1,2-cis fashion<sup>22,23,41,42</sup>.

Closer scrutiny of these transition structures showed important non-covalent H-bond interactions between catalysts and reactants. In **TS-I**, the pyrrolidine unit in **16K** forms a H-bond with the C3-OH of donor **15**. This C3-OH then forms a H-bond with the Br leaving group, assisting with its cleavage. Such an arrangement oriented the axial C4-OH in acceptor **11** closest to the electrophilic centre, resulting in **12a** with unusual site selectivity. Another transition structure, **TS-II**, was also found to favour **12a**, in which the pyrrolidine ring in **16K** formed the H-bond with the C2-OH of acceptor **11**, thereby exposing the C4-OH of **11** maximally. The availability of two low-energy transition structures (**TS-I** and **-II**) aligns with the observation that blocking of either the C3-OH of donor **10** or the C2-OH of acceptor **11** does not dramatically compromise site selectivity (Extended Data Fig. 4a). If both of these sites are obstructed, however, a marked decrease in selectivity occurs (28% overall yield, 3:1 ratio; Supplementary Fig. 9). For catalyst **16M**, **TS-III** was located. In this case, the N atom in **16M** cannot reach hydroxyl groups other than those bound to boron due to the short distance between the N and B atoms. As a result the C3-OH in acceptor **11**, which is equatorial and presumably more nucleophilic, is glycosylated selectively. Not unexpectedly, for catalyst **16M**, neither the C2-OH in acceptor **11** nor the C3-OH in donor **10** was crucial for site selectivity (Extended Data Fig. 4a). Preliminary as these are, our models could potentially lay the foundation for the development of catalysts to generate products with other types of linkage.

## Conclusion

We developed a general platform that accomplishes site-, stereo- and chemoselective O-glycosylation between minimally protected donors and acceptors. The strategy operates on a radical-based donor activation system that generates electrophilic glycosyl bromides under mild conditions, allowing the application of designed aminoboronic acid catalysts to control the trajectory of subsequent glycosyl transfer to acceptors. Experimental and computational studies suggest that catalysts function by organizing donors and acceptors in proximity through reversible covalent B–O bonds and non-covalent H-bond interactions. The method affords the challenging 1,2-cis-O-glycosidic bonds in a site-switchable manner: the reaction site can be switched through alteration of the catalyst structure. In the reactions developed, most acceptors contained the cis-1,2-diol unit (to chelate with the boron atom in the catalysts) and 1,2-cis-glycosylation occurred within such units. The generality and potential utility of this strategy are demonstrated in the synthesis of intricate oligosaccharides and naturally existing sugar chains. This study showcases a straightforward stage in the design of protecting-group-independent, catalyst-controlled glycosylation reactions, which would ultimately simplify oligosaccharide synthesis and facilitate the exploration of carbohydrate functions.

## Online content

Any methods, additional references, Nature Portfolio reporting summaries, source data, extended data, supplementary information,

acknowledgements, peer review information; details of author contributions and competing interests; and statements of data and code availability are available at <https://doi.org/10.1038/s41586-024-07695-4>.

- Varki, A. et al. *Essentials of Glycobiology* (Cold Spring Harbor Laboratory Press, 2022).
- Barchi, J. J., Jr. *Comprehensive Glycoscience: From Chemistry to Systems Biology* (Elsevier, 2021).
- Demchenko, A. V. *Handbook of Chemical Glycosylation* (Wiley-VCH, 2008).
- Werz, D. B. & Vidal, S. *Modern Synthetic Methods in Carbohydrate Chemistry: From Monosaccharides to Complex Glycoconjugates* (Wiley-VCH, 2014).
- Guo, J. & Ye, X.-S. Protecting groups in carbohydrate chemistry: influence on stereoselectivity of glycosylations. *Molecules* **15**, 7235–7265 (2010).
- Vidal, S. *Protecting Groups: Strategies and Applications in Carbohydrate Chemistry* (Wiley-VCH, 2019).
- Hettikankanalage, A. A., Lassfolk, R., Ekholm, F. S., Leino, R. & Crich, D. Mechanisms of stereodirecting participation and ester migration from near and far in glycosylation and related reactions. *Chem. Rev.* **120**, 7104–7151 (2020).
- Bennett, C. S. *Selective Glycosylations: Synthetic Methods and Catalysts* (Wiley-VCH, 2017).
- Shang, W. & Niu, D. Radical pathway glycosylation empowered by bench-stable glycosyl donors. *Acc. Chem. Res.* **56**, 2473–2488 (2023).
- Danishfsky, S. J., Shue, Y.-K., Chang, M. N. & Wong, C.-H. Development of globo-H cancer vaccine. *Acc. Chem. Res.* **48**, 643–652 (2015).
- Yu, B., Sun, J. & Yang, X. Assembly of naturally occurring glycosides, evolved tactics, and glycosylation methods. *Acc. Chem. Res.* **45**, 1227–1236 (2012).
- Panza, M., Pistorio, S. G., Stine, K. J. & Demchenko, A. V. Automated chemical oligosaccharide synthesis: Novel approach to traditional challenges. *Chem. Rev.* **118**, 8105–8150 (2018).
- Seegerber, P. H. The logic of automated glycan assembly. *Acc. Chem. Res.* **48**, 1450–1463 (2015).
- Yao, W. et al. Automated solution-phase multiplicative synthesis of complex glycans up to a 1,080-mer. *Nat. Synth.* **1**, 854–863 (2022).
- Young, I. & Baran, P. Protecting-group-free synthesis as an opportunity for invention. *Nat. Chem.* **1**, 193–205 (2009).
- Shugrue, C. R. & Miller, S. J. Applications of nonenzymatic catalysts to the alteration of natural products. *Chem. Rev.* **117**, 11894–11951 (2017).
- Witte, M. D. & Minnaard, A. J. Site-selective modification of (oligo)saccharides. *ACS Catal.* **12**, 12195–12205 (2022).
- Yamatsugu, K. & Kanai, M. Catalytic approaches to chemo- and site-selective transformation of carbohydrates. *Chem. Rev.* **123**, 6793–6838 (2023).
- Oshima, K. & Aoyama, Y. Regiospecific glycosidation of unprotected sugars via arylboronic activation. *J. Am. Chem. Soc.* **121**, 2315–2316 (1999).
- Dimakos, V. & Taylor, M. S. Site-selective functionalization of hydroxyl groups in carbohydrate derivatives. *Chem. Rev.* **118**, 11457–11517 (2018).
- Taylor, M. S. Catalysis based on reversible covalent interactions of organoboron compounds. *Acc. Chem. Res.* **48**, 295–305 (2015).
- Tanaka, M. et al. Boronic-acid-catalyzed regioselective and 1,2-cis-stereoselective glycosylation of unprotected sugar acceptors via S<sub>n</sub>i-type mechanism. *J. Am. Chem. Soc.* **140**, 3644–3651 (2018).
- Takahashi, D., Inaba, K. & Toshima, K. Recent advances in boron-mediated aglycon delivery (BMAD) for the efficient synthesis of 1,2-cis glycosides. *Carbohydr. Res.* **518**, 108579–108588 (2022).
- Li, Q., Levi, S. M., Wagen, C. C., Wendlandt, A. E. & Jacobsen, E. N. Site-selective, stereocontrolled glycosylation of minimally protected sugars. *Nature* **608**, 74–79 (2022).
- Levi, S. M. & Jacobsen, E. N. Catalyst-controlled glycosylations. *Org. React.* **100**, 801–852 (2019).
- Wadzinski, T. J. et al. Rapid phenolic O-glycosylation of small molecules and complex unprotected peptides in aqueous solvent. *Nat. Chem.* **10**, 644–652 (2018).
- Pelletier, G., Zwicker, A., Allen, C. L., Schepartz, A. & Miller, S. J. Aqueous glycosylation of unprotected sucrose employing glycosyl fluorides in the presence of calcium ion and trimethylamine. *J. Am. Chem. Soc.* **138**, 3175–3182 (2016).
- Loh, C. C. J. Exploiting non-covalent interactions in selective carbohydrate synthesis. *Nat. Rev. Chem.* **5**, 792–815 (2021).
- Shang, W., He, B. & Niu, D. Ligand-controlled, transition-metal catalyzed site-selective modification of glycosides. *Carbohydr. Res.* **474**, 17–33 (2019).
- Loh, C. C. J. Synergistic catalysis: an emerging concept for selective carbohydrate synthesis. *Chem. Catal.* **4**, 100891–100902 (2024).
- Rao, V. U. B. et al. A synergistic Rh(I)/organoboron-catalysed site-selective carbohydrate functionalization that involves multiple stereocontrol. *Nat. Chem.* **15**, 424–435 (2023).
- Wang, G. et al. Bond editing of unprotected saccharides. *J. Am. Chem. Soc.* **146**, 824–832 (2024).
- Wang, Y., Carder, H. M. & Wendlandt, A. E. Synthesis of rare sugar isomers through site-selective epimerization. *Nature* **578**, 403–408 (2020).
- Zhang, C. et al. Halogen-bond-assisted radical activation of glycosyl donors enables mild and stereoconvergent 1,2-cis-glycosylation. *Nat. Chem.* **14**, 686–694 (2022).
- Huang, Z. & Dong, G. Site-selectivity control in organic reactions: a quest to differentiate reactivity among the same kind of functional groups. *Acc. Chem. Res.* **50**, 465–471 (2017).
- Toste, F. D., Sigman, M. S. & Miller, S. J. Pursuit of noncovalent interactions for strategic site-selective catalysis. *Acc. Chem. Res.* **50**, 609–615 (2017).
- Lemieux, R. U., Hendriks, K. B., Stick, R. V. & James, K. Halide ion catalyzed glycosidation reactions. Syntheses of alpha-linked disaccharides. *J. Am. Chem. Soc.* **97**, 4056–4062 (1975).
- Diehl, K. L. et al. Design and synthesis of synthetic receptors for biomolecule recognition. *Monogr. Supramol. Chem.* **14**, 39–85 (2015).

39. Bull, S. D. et al. Exploiting the reversible covalent bonding of boronic acids: recognition, sensing, and assembly. *Acc. Chem. Res.* **46**, 312–326 (2013).
40. Yasomanee, J. P. & Demchenko, A. V. Effect of remote picolinyl and picoloyl substituents on the stereoselectivity of chemical glycosylation. *J. Am. Chem. Soc.* **134**, 20097–20102 (2012).
41. Nigudkar, S. S. & Demchenko, A. V. Stereocontrolled 1,2-cis glycosylation as the driving force of progress in synthetic carbohydrate chemistry. *Chem. Sci.* **6**, 2687–2704 (2015).
42. Mensink, R. A. & Boltje, T. J. Advances in stereoselective 1,2-cis glycosylation using C-2 auxiliaries. *Chem. Eur. J.* **23**, 17637–17653 (2017).
43. Chang, C.-W. et al. Automated quantification of hydroxyl reactivities: prediction of glycosylation reactions. *Angew. Chem. Int. Ed. Engl.* **60**, 12413–12423 (2021).
44. van der Vorm, S. et al. Acceptor reactivity in glycosylation reactions. *Chem. Soc. Rev.* **48**, 4688–4706 (2019).
45. Chatterjee, S., Moon, S., Hentschel, F., Gilmore, K. & Seeberger, P. H. An empirical understanding of the glycosylation reaction. *J. Am. Chem. Soc.* **140**, 11942–11953 (2018).
46. Crich, D. Mechanism of a chemical glycosylation reaction. *Acc. Chem. Res.* **43**, 1144–1153 (2010).
47. Georgiou, I., Ilyashenko, G. & Whiting, A. Synthesis of aminoboronic acids and their applications in bifunctional catalysis. *Acc. Chem. Res.* **42**, 756–768 (2009).
48. Singh, Y., Geringer, S. A. & Demchenko, A. V. Synthesis and glycosidation of anomeric halides: evolution from early studies to modern methods of the 21st century. *Chem. Rev.* **122**, 11701–11758 (2022).

**Publisher's note** Springer Nature remains neutral with regard to jurisdictional claims in published maps and institutional affiliations.

Springer Nature or its licensor (e.g. a society or other partner) holds exclusive rights to this article under a publishing agreement with the author(s) or other rightsholder(s); author self-archiving of the accepted manuscript version of this article is solely governed by the terms of such publishing agreement and applicable law.

© The Author(s), under exclusive licence to Springer Nature Limited 2024

# Article

## Methods

To an 8 ml screw-capped glass vial containing a magnetic stir bar were sequentially added allyl glycosyl sulfone (0.2 mmol, 1.0 equiv.), sugar acceptor (0.3–0.4 mmol, 1.5–2.0 equiv.), *fac*-Ir(ppy)<sub>3</sub> (0.004 mmol, 2 mol%), (NH<sub>4</sub>)<sub>2</sub>HPO<sub>4</sub> (0.6 mmol, 3.0 equiv.), aminoboronic acid catalyst (0.04 mmol, 0.2 equiv.), BrCF<sub>2</sub>COOEt (0.6 mmol, 3.0 equiv.) and EtOAc (3.0 ml) under a N<sub>2</sub> atmosphere. The vial was tightly sealed by a Teflon-lined cap, and allowed to stir at room temperature for the indicated period of time, with a 10 W (455 nm) light-emitting diode bulb placed about 3 cm below. The reaction mixture was concentrated under reduced pressure and the residue was purified using either (1) reverse-phase column chromatography (H<sub>2</sub>O:MeCN or MeOH:MeCN) using a Biotage Isolera One equipped with a Spherial C<sub>18</sub> column (25–40 µm, 100 Å, 114 × 12.4 mm<sup>2</sup>) or (2) silica gel chromatography.

## Data availability

Experimental details and characterization data supporting the findings of this study are available within the paper and its Supplementary Information and from the Cambridge Crystallographic Data Centre

(<https://www.ccdc.cam.ac.uk/structures>; crystallographic data are available under CCDC reference nos. CCDC 2303235, 2303244, 2303245, 2303249 and 2322042).

**Acknowledgements** We acknowledge financial support by the National Natural Science Foundation of China (grant nos. 21922106, 21933004 and T2221004) and the 1.3.5 Project for Disciplines of Excellence, West China Hospital. We thank H. Wang from the Mass Spectrometry Core Facility at the College of Life Sciences, Sichuan University for assistance with mass spectral analysis, and X. Wang from the Analytical and Testing Center, Sichuan University for assistance with NMR analysis.

**Author contributions** D.N. conceived the idea, guided the project and wrote the manuscript, with feedback from other authors. Q.-D.D. recorded the initial observations and analysed results. Q.-D.D., Y.Z., J.L. and X.Z. explored substrate scope and performed mechanistic studies. Y.-H.D. and T.-Y.S. performed DFT calculations on the reaction mechanism and made suggestions on improving the catalyst, with advice from Y.-D.W.

**Competing interests** The authors declare no competing interests.

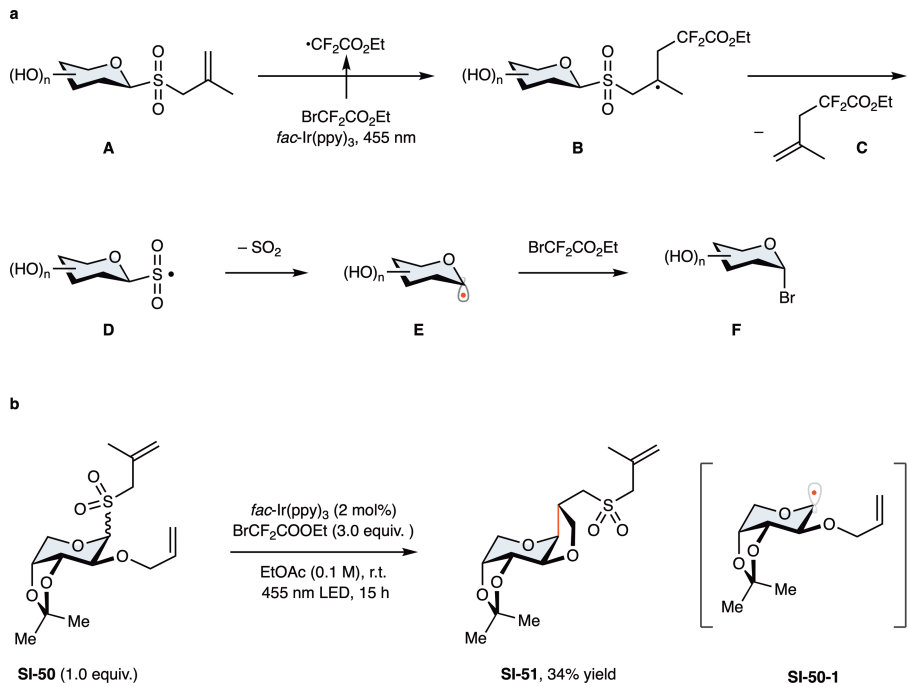
### Additional information

**Supplementary information** The online version contains supplementary material available at <https://doi.org/10.1038/s41586-024-07695-4>.

**Correspondence and requests for materials** should be addressed to Yun-Dong Wu or Dawen Niu.

**Peer review information** *Nature* thanks Charles C. J. Loh and the other, anonymous, reviewer(s) for their contribution to the peer review of this work. Peer reviewer reports are available.

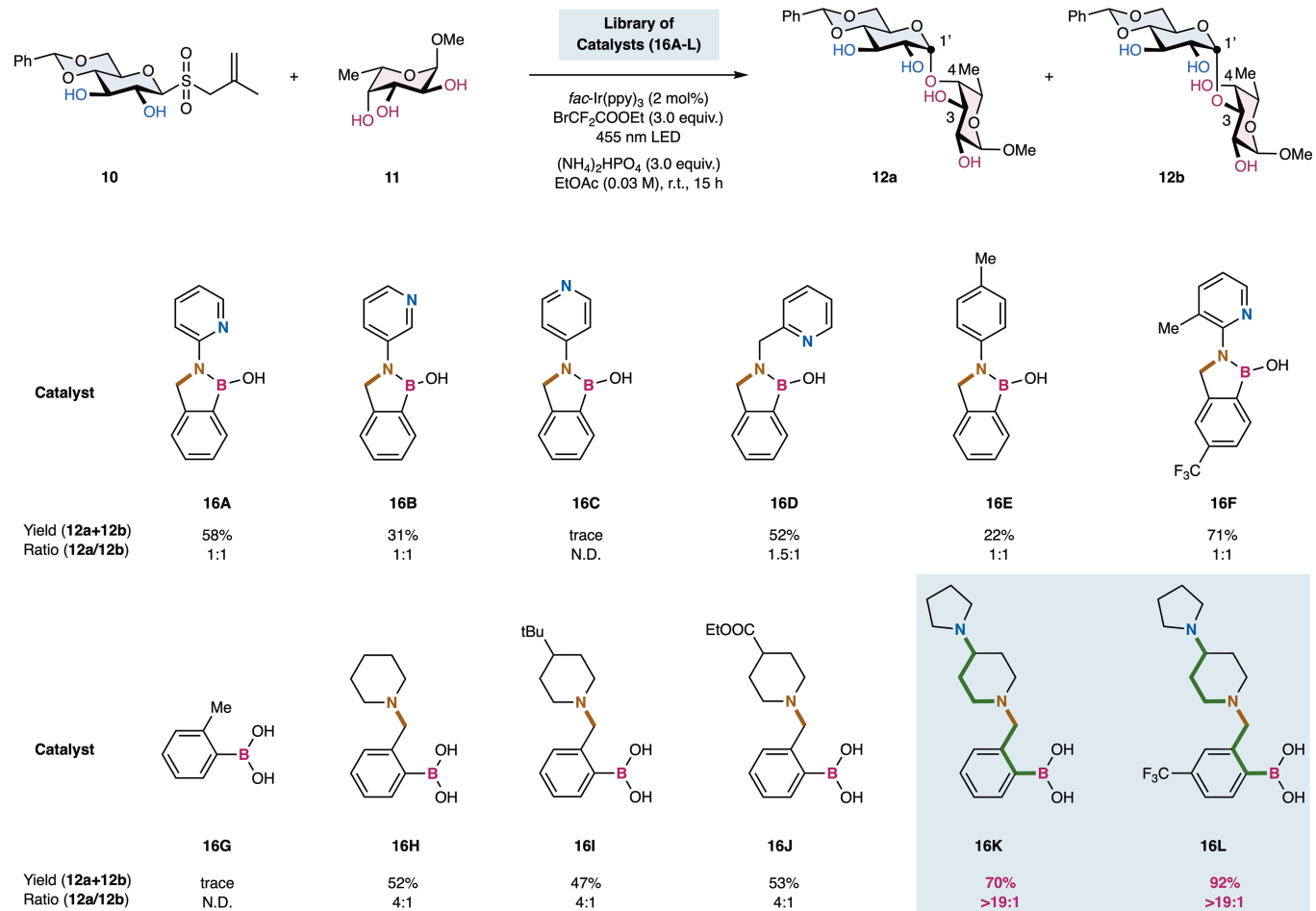
**Reprints and permissions information** is available at <http://www.nature.com/reprints>.



**Extended Data Fig. 1 | Mechanism for the generation of glycosyl bromides from allyl glycosyl sulfones.** **a**, Proposed mechanism for the generation of glycosyl bromides. Photoexcited *fac*-Ir(ppy)<sub>3</sub> could reduce BrCF<sub>2</sub>CO<sub>2</sub>Et to give •CF<sub>2</sub>CO<sub>2</sub>Et. This species then attacks terminal alkene group in sulfone **A** to give alkyl radical **B**, which ejects alkene **C** (to from **D**) and then SO<sub>2</sub> to give glycosyl

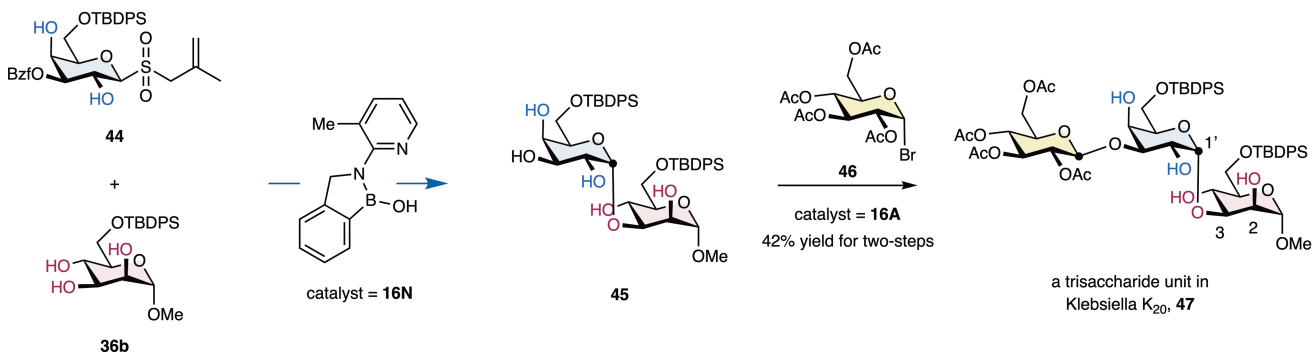
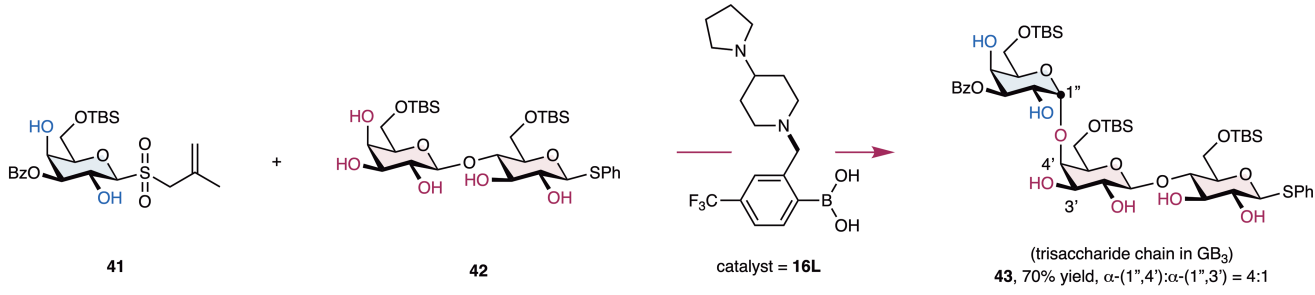
radical **E**. Bromide transfer from BrCF<sub>2</sub>CO<sub>2</sub>Et to **E** affords glycosyl bromide **F**. **b**, Support for the intermediacy of glycosyl radicals. We designed sulfone **SI-50**. Irradiation of **SI-50** under 455 nm LED in the presence of *fac*-Ir(ppy)<sub>3</sub> and BrCF<sub>2</sub>CO<sub>2</sub>Et gave cyclized product **SI-51** in decent yield, supporting the intermediacy of **SI-50-1**.

# Article



**Extended Data Fig. 2 | Evaluation of catalysts performance.** The model reaction employs minimally protected donor **10** and acceptor **11**. Product ratios were determined by <sup>1</sup>H NMR analysis of crude reaction mixture. Reactions

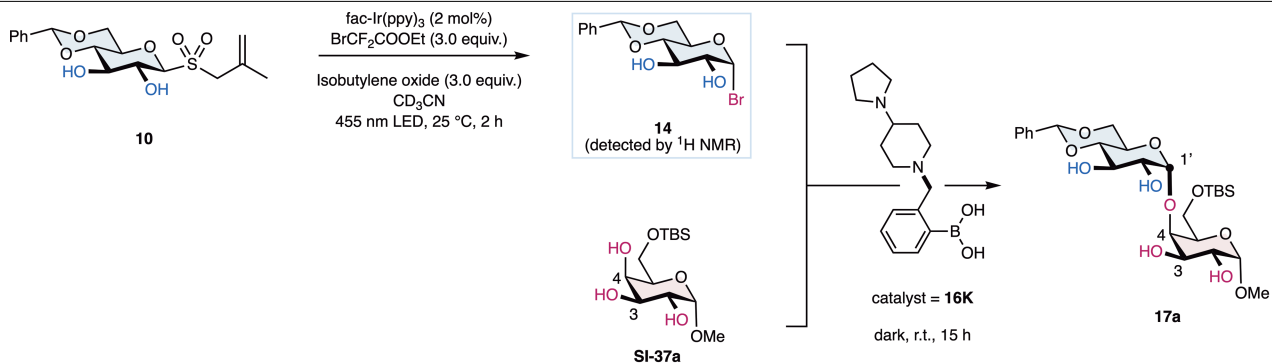
were performed at 0.05 mmol scale in EtOAc (0.03 M) for 15 h, using *fac*-Ir(ppy)<sub>3</sub> (2 mol%), BrCF<sub>2</sub>CO<sub>2</sub>Et (3.0 equiv.), (NH<sub>4</sub>)<sub>2</sub>HPO<sub>4</sub> (3.0 equiv.) and a catalyst (0.2 equiv.).



**Extended Data Fig. 3 | Synthetic application.** Reactions in this Figure were performed at 0.1 or 0.2 mmol scale in EtOAc (0.03 M) for 15 h, using *fac*-Ir(ppy)<sub>3</sub> (2 mol%), BrCF<sub>2</sub>CO<sub>2</sub>Et (3.0 equiv.), (NH<sub>4</sub>)<sub>2</sub>HPO<sub>4</sub> (3.0 equiv.), and the indicated

catalyst. The product ratios were determined by <sup>1</sup>H NMR analysis of crude reaction mixture. Isolated yields are reported. See SI for experimental details.

# Article

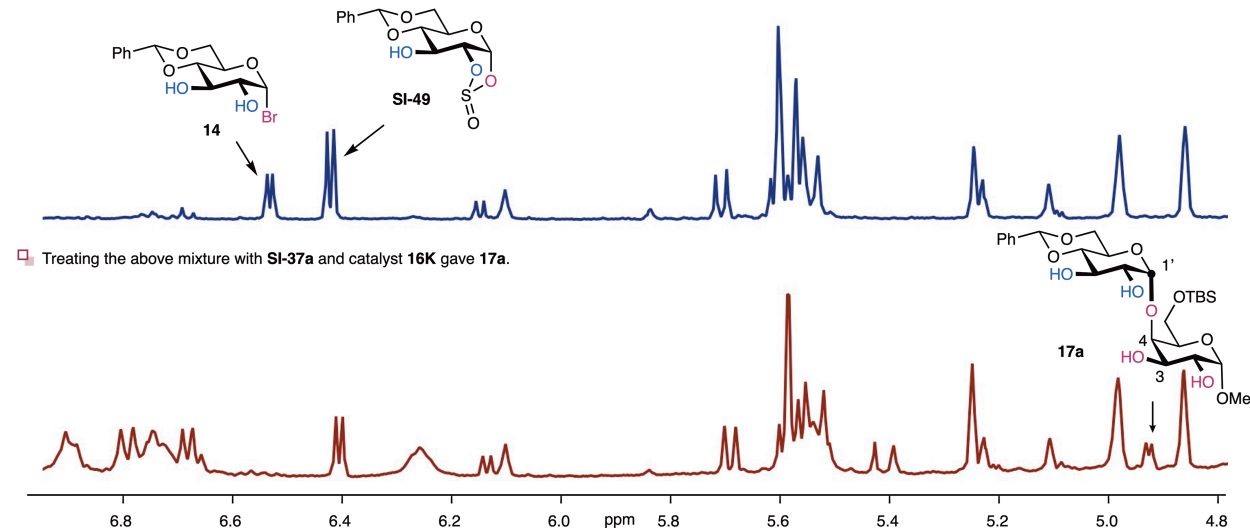


□ Allyl glycosyl sulfone **10**



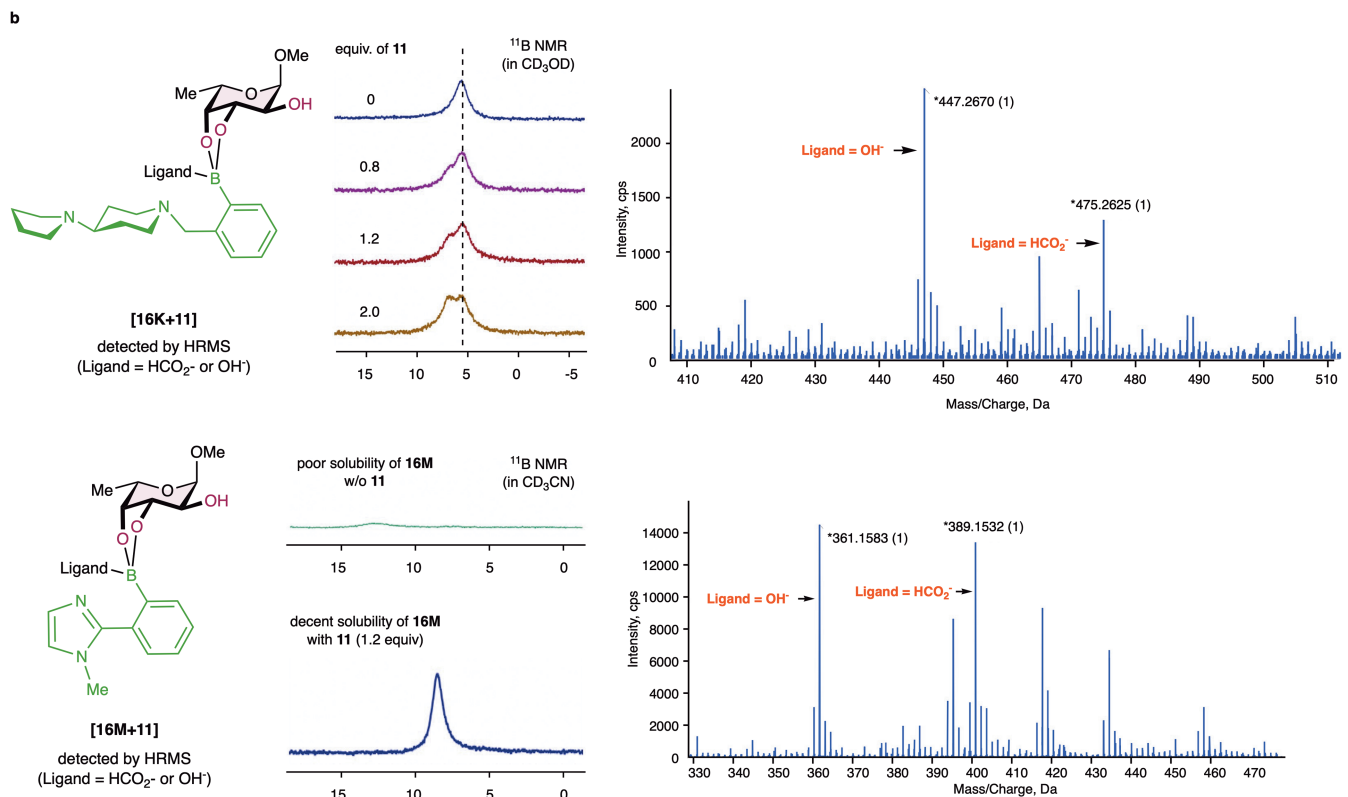
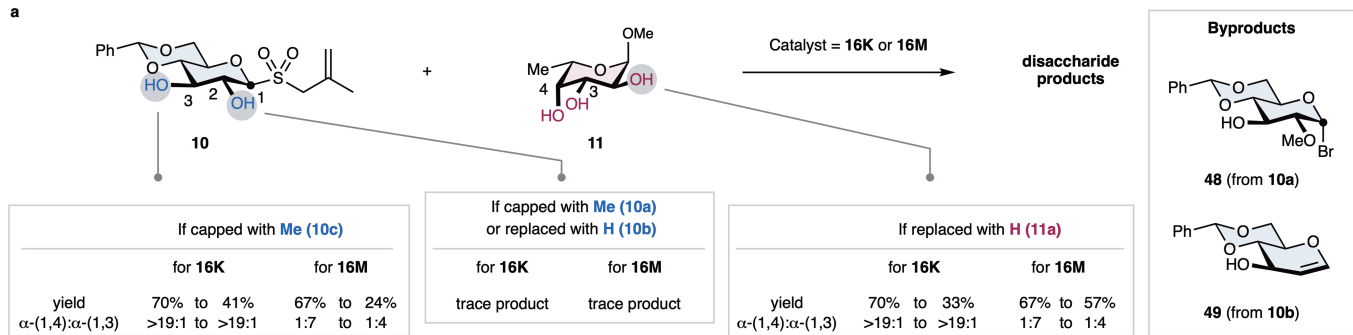
<sup>1</sup>H NMR  
400 MHz, CD<sub>3</sub>CN

□ Irradiating **10** at 455 nm for 2 h in the presence of BrCF<sub>2</sub>CO<sub>2</sub>Et and fac-Ir(ppy)<sub>3</sub> afforded **14** and **SI-49**.



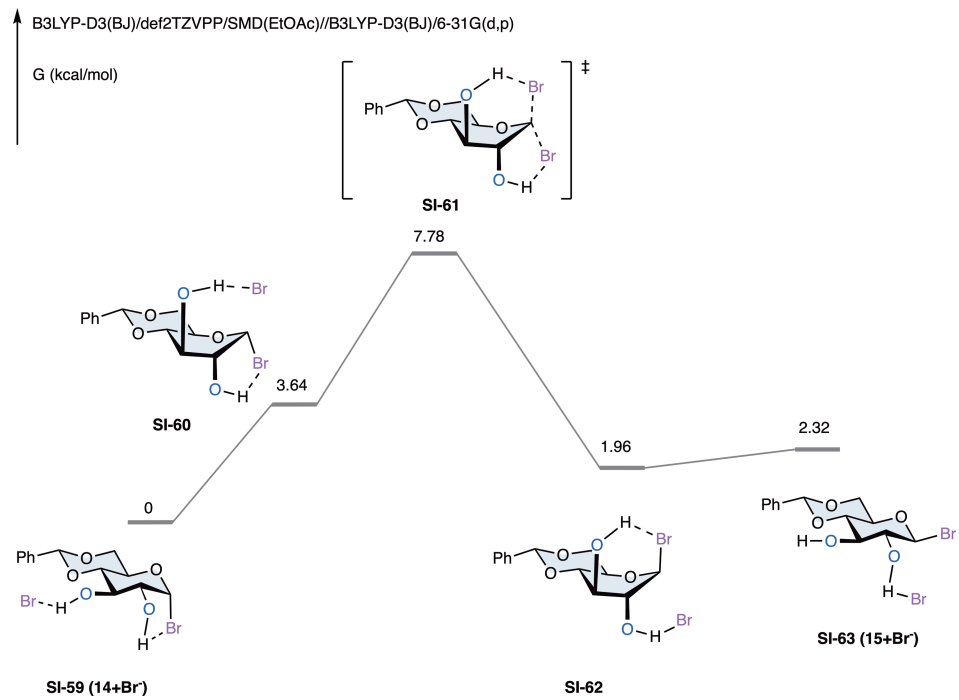
**Extended Data Fig. 4 | Mechanistic studies.** **a**, Controlled experiments using donors and acceptors with perturbed structures. Reactions were performed at 0.1 mmol scale in EtOAc (0.03 M) for 15 h, using *fac*-Ir(ppy)<sub>3</sub> (2 mol%), BrCF<sub>2</sub>CO<sub>2</sub>Et (3.0 equiv.), (NH<sub>4</sub>)<sub>2</sub>HPO<sub>4</sub> (3.0 equiv.), and catalyst **16K** or **16M**

(0.2 equiv.). **b**, Complexation between catalysts and acceptor **11**. The boron atoms in the complexes presumably bear four ligands, given their chemical shifts. Existence of [**16K+11**] or [**16M+11**] was detected by mass spectrometry. See SI for experimental details.



**Extended Data Fig. 5 | Generation, detection and reaction of glycosyl bromide intermediate.** We performed our reaction using  $\text{CD}_3\text{CN}$  as solvent, in order to monitor the progress by  $^1\text{H}$  NMR. In the absence of catalyst and acceptor, irradiating allyl glycosyl sulfone **10** under 455 nm LED with *fac*-Ir(*ppy*)<sub>3</sub>,  $\text{BrCF}_3\text{COEt}$ , and isobutylene oxide as acid scavenger for 2 h gave

glycosyl bromide **14** detectable by  $^1\text{H}$  NMR. During the process **SI-49** was formed as a byproduct, whose structure was verified by X-ray crystallography (CCDC No. 2303244). Adding acceptor **SI-37a** and catalyst **16K** to the above mixture converted **14** to product **1a**. These results support glycosyl bromides are generated as intermediates and serve as reactive electrophiles.



**Extended Data Fig. 6 | A potential epimerization pathway between axially and equatorially configured glycosyl bromides.** As anticipated, the epimerization between axially and equatorially configured glycosyl bromides occurred in a facile manner. For example, the conversion between **SI-59** and

**SI-63** was computed to have a small energy barrier. DFT calculations were performed at B3LYP-D3(BJ)/def2TZVPP/SMD(EtOAc)//B3LYP-D3(BJ)/6-31G(d,p) level of theory.